MRS Advances
https://doi.org/10.1557/s43580-024-00877-2

ORIGINAL PAPER

Influence of reactant properties in deposition of silicon oxycarbide thin films by hot filament chemical vapor deposition

Ivan Enrique Garcia Balderas[1] · Alexander Petrovich Kondratov[1]

Received: 16 February 2024 / Accepted: 7 May 2024

Abstract

This research investigates the properties of silicon oxycarbide thin films obtained by Hot Filament Chemical Vapor Deposition, utilizing tetraethoxysilane and MCM-41 as reactants. A comprehensive analysis of the influence of MCM-41 on thin-film properties is conducted by systematically varying its quantities (5, 10, and 15 g). Energy-dispersive X-ray analysis shows the presence of carbon, oxygen, and silicon, consistent with the use of TEOS and MCM-41. Microscopic examination reveals distinct morphologies in the silicon oxycarbide thin films; when only TEOS is employed, the surface exhibits compact aggregates heterogeneously distributed, while the introduction of both TEOS and MCM-41 results in porous clusters. Furthermore, the presence of MCM-41 enhances photoluminescence in the thin films, suggesting quantum confinement effects. This study provides valuable insights into the synergistic interplay between TEOS and MCM-41, offering opportunities for optimizing silicon oxycarbide thin films for a range of applications spanning from microelectronics to optoelectronics.

Introduction

Silicon oxycarbide (SiOC) has garnered significant attention in materials science due to its properties and possible applications [1–3]. This material, composed of silicon, oxygen, and carbon, offers a unique combination of mechanical, thermal, optical, and electrical characteristics, making it highly useful for a wide range of applications across various industries [4–6]. SiOC's ability to be tailored at the molecular level allows for precise control over its properties, enabling the design materials with specific functionalities to meet diverse technological needs [7–9].

Its mechanical strength, hardness, and toughness make it suitable for structural applications requiring durability and resilience, while its thermal stability and conductivity enable effective heat dissipation in high-temperature environments. SiOC's optical properties, including transparency and tunable refractive index, offer opportunities for use in photonics and optical coatings, facilitating advancements in telecommunications and imaging technologies. Additionally, SiOC exhibits chemical stability and biocompatibility, making it suitable for applications in harsh chemical environments and biomedical devices. Its electrical properties, such as dielectric constant and conductivity, further enhance its utility in electronics and semiconductor applications [4–6].

Silicon oxycarbide thin films deposited by Hot Filament Chemical Vapor Deposition (HFCVD) represent a promising material. Precise control of their properties is essential, and the selection of precursor materials plays a crucial role in influencing composition, structure, and performance. Tetraethoxysilane (TEOS) is a widely studied precursor for SiOC film synthesis due to its controlled decomposition and contribution to the Si–O–C network [10]. Concurrently, the incorporation of MCM-41 introduces new possibilities to the deposition process. MCM-41, characterized by its unique mesoporous structure, offers opportunities to influence thin-film properties. This investigation delves into the synergistic impact of MCM-41 and TEOS as reactants in the HFCVD process for SiOC thin-film synthesis. By systematically varying MCM-41 quantities (ranging from 5 to 15 g) and comparing against exclusive TEOS deposition, the study aims to elucidate their influence on resulting thin-film properties. The selected concentrations allow exploration of dose-dependent effects of MCM-41 and assessment of its potential in modulating thin-film composition, morphology, and functional properties.

✉ Ivan Enrique Garcia Balderas
ivanegarciab@gmail.com

[1] Moscow Polytechnic University, 38 Bolshaya Semenovskaya Street, Moscow, Russia 127008

Published online: 15 May 2024

This study aims to offer a comprehensive understanding of the interplay between TEOS and MCM-41 in SiOC thin-film deposition, with implications for process optimization, enhanced thin-film properties, and tailored applications in advanced materials and device technologies, spanning from microelectronics to optoelectronics.

Materials and methods

Methodology

Thin silicon oxycarbide films were obtained by Hot Filament Chemical Vapor Deposition (HFCVD) method, employing two different reactant configurations:

(a) Exclusive use of tetraethoxysilane (TEOS).
(b) Combination of TEOS and mesoporous silica granules MCM-41.

The quantity of MCM-41 introduced into the deposition process was varied across three different concentrations: 5 g, 10 g, and 15 g. The deposition process took place within a low-vacuum chamber with a base pressure of 14 kPa.

MCM-41 granules were synthesized following an established methodology [11]. To minimize direct oxygen reactions on the hot filament surface, hydrogen was employed as a carrier gas due to its higher reactivity compared to oxygen [12]. A hydrogen flow rate of 100 sccm was maintained throughout the process.

Thin films were deposited onto p-type silicon substrates, each having a thickness of 279 ± 20 µm and a resistivity ranging from 1 to 10 Ω•cm. The substrates underwent thorough pre-cleaning procedures following the Radio Corporation of America RCA I and RCA II protocols [13, 14].

During the deposition process, 25 ml of TEOS were introduced into a two-tube flask, with one tube connected to a high-purity gaseous hydrogen tank, and the other leading to the reactor's reaction chamber. Gaseous hydrogen passed through the flask, bubbling through the liquid TEOS. The resulting gas, a mixture of TEOS vapor and hydrogen, entered the reaction chamber where it underwent dissociation facilitated by the heated tungsten filament acting as a catalyst.

The filament's temperature was precisely controlled at 1800 °C using a variable autotransformer (VARIAC). Figure 1a shows a diagram of the HFCVD system components. The schematic representation in Fig. 1b shows the components within the reaction chamber.

The filament's temperature was precisely controlled at 1800 °C using a variable autotransformer (VARIAC). In the gas phase, TEOS molecules underwent dissociation with the assistance of the heated tungsten filament. Concurrently, hydrogen molecules (H2) were catalytically cracked on the filament, producing free hydrogen radicals (H). Positioned 4 mm away from the filament, MCM-41 granules were exposed to these free hydrogen radicals, leading to the formation of silicon oxide particles. These particles underwent adsorption, initiated nucleation, and subsequently grew on the substrate, contributing to a higher SiOx content in the chemical composition of the resulting films.

Characterization techniques

The silicon oxycarbide thin films underwent comprehensive characterization using advanced analytical techniques.

Scanning electron microscopy (SEM) was conducted using an Auriga 3916-FESEM operated at 1 kV, facilitating high-resolution imaging for surface morphology and structural analysis.

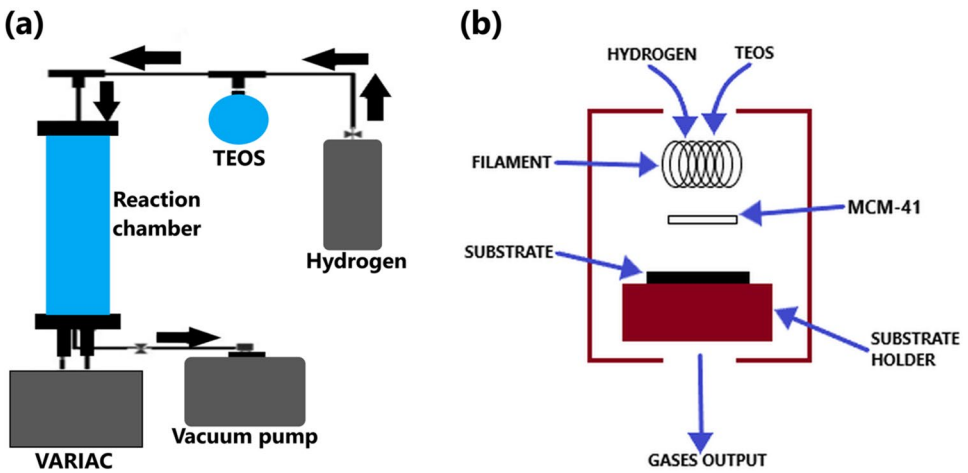

Fig. 1 **a** Diagram of the HFCVD system components. **b** Diagram of the components inside the reaction chamber of the HFCVD system

Energy-Dispersive X-Ray (EDS) spectra were acquired on the same Auriga 3916-FESEM, with an accelerating voltage range of 1 to 3 keV, to perform elemental analysis.

For the evaluation of optical properties, photoluminescence spectroscopy was employed. This analysis utilized a Fluoromax-3 fluorescence spectrophotometer equipped with a 150-W xenon lamp and an R928P photomultiplier tube as the signal detector. The measurements were conducted at 20 °C, with an excitation wavelength of 330-nm and a 370-nm filter.

Results

Energy-dispersive X-ray spectroscopy

Figure 2 shows the energy-dispersive X-ray spectra, providing a comprehensive analysis of the chemical composition of silicon oxycarbide thin films obtained by Hot Filament Chemical Vapor Deposition.

These thin films were prepared using two distinct sets of reactants:

(a) Solely tetraethoxysilane (TEOS) and
(b) A combination of TEOS and 15 g of MCM-41 as reactants.

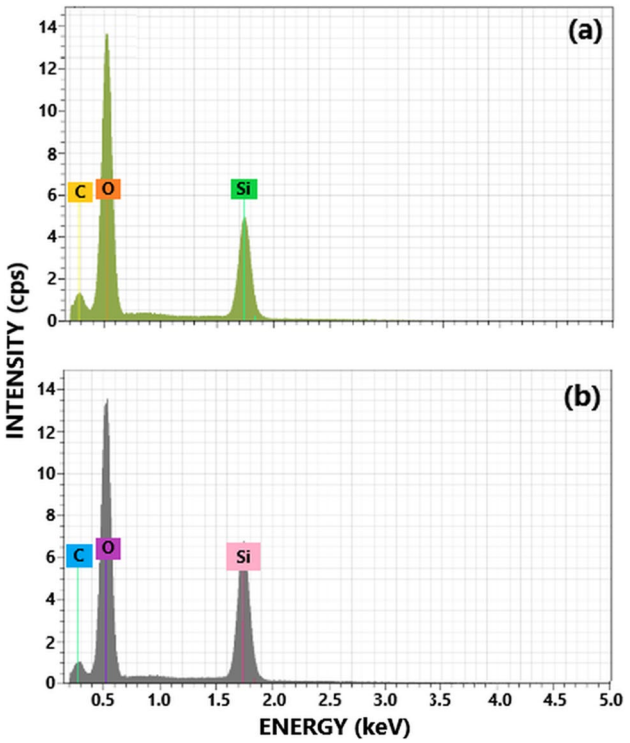

Fig. 2 EDS spectra of silicon oxycarbide thin films using **a** only TEOS and **b** TEOS and MCM-41 as reactants

Scanning electron microscopy

Figure 3 shows Field-Emission Scanning Electron Micrographs (FE-SEM) depicting silicon oxycarbide thin films obtained by Hot Filament Chemical Vapor Deposition, utilizing two distinct reactant configurations:

(a) Exclusive use of tetraethoxysilane.
(b) Combination of TEOS and 15 g of MCM-41.

Figure 3a1 offers an enlarged perspective of Fig. 3a, magnifying details with a factor of 50.00 KX.

Figure 3b1 provides an amplified view of Fig. 3b, also at a magnification factor of 50.00 KX, focusing particularly on the clusters within the SiOC thin films.

Photoluminescence

Figure 4 illustrates the photoluminescence spectra of SiOC thin films obtained by Hot Filament Chemical Vapor Deposition. Two different deposition routes were employed:

(a) Exclusively utilizing Tetraethylorthosilicate.
(b) Incorporating TEOS with varying amounts of MCM-41 (5 g, 10 g, and 15 g) as precursors.

Discussion

Energy-dispersive X-ray spectroscopy

The findings presented in Fig. 2 show the elemental constituents within the thin films, carbon, oxygen, and silicon. This elemental composition aligns with the use of TEOS (Si(OC2H5)4) and MCM-41 (SiO2) as precursors [15, 16]. The identification of carbon, oxygen, and silicon in the spectra affirms the formation of silicon oxycarbide, indicating the successful integration of chemical elements from the precursors.

The presence of carbon in the films originates from the introduction of organosilicon precursors, particularly TEOS, which contains ethoxy (OC2H5) groups [17]. Throughout the HFCVD process, these organic groups undergo decomposition, actively contributing to the establishment of the Si–O–C network. This process results in the incorporation of carbon into the thin films, influencing their distinctive composition and properties.

Oxygen, an essential component of both TEOS and mesoporous silica granules, is expected to be a prominent constituent in the SiOC films. The chemical interactions occurring during the HFCVD process give rise to the formation of Si–O–Si and Si–O–C bonds. These bonds significantly contribute to the observed oxygen content, highlighting the crucial role of oxygen in forming the chemical structure of the silicon oxycarbide thin films.

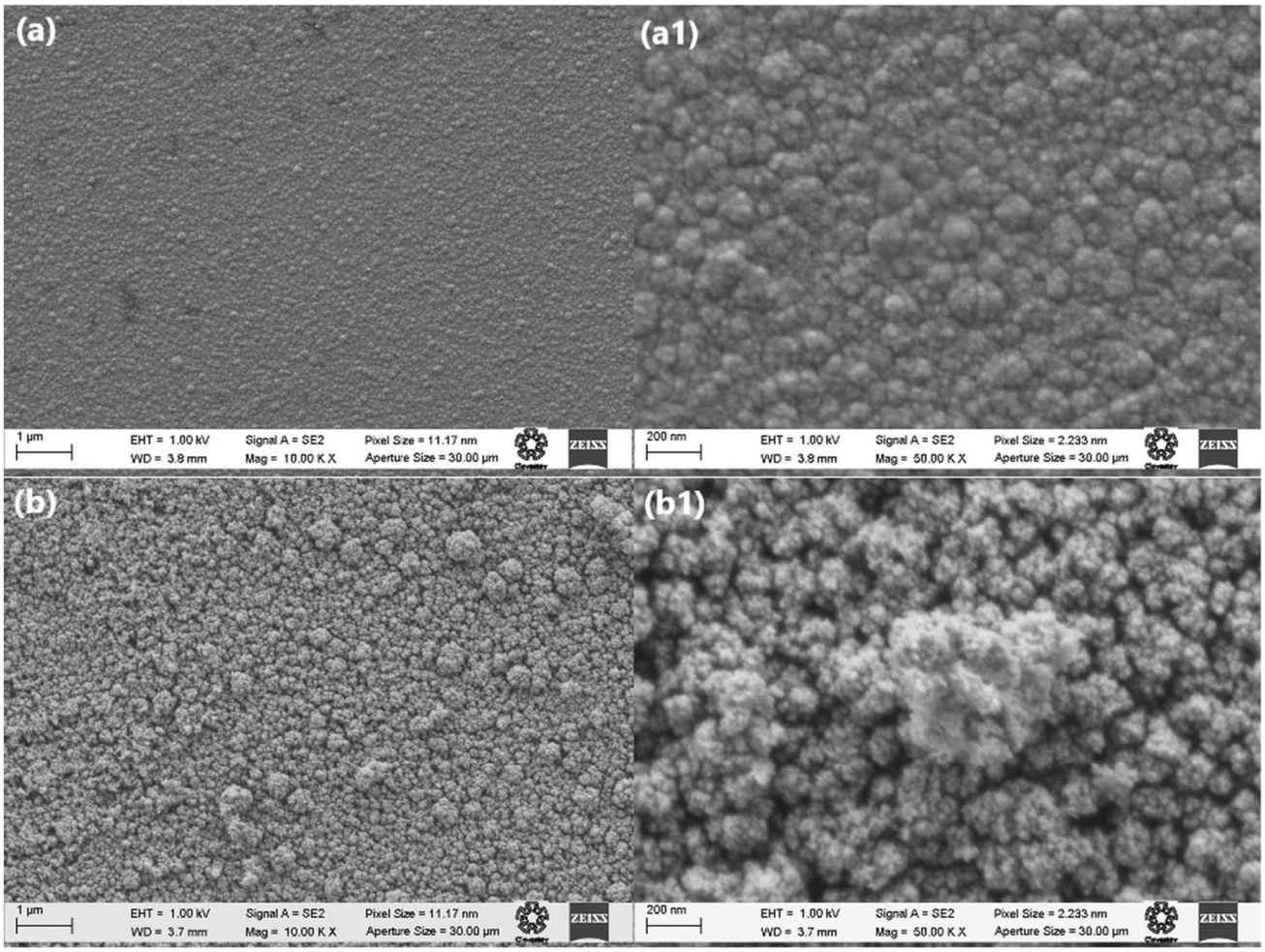

Fig. 3 FE-SEM micrographs of silicon oxycarbide thin films prepared by HFCVD using **a** only TEOS with a1 corresponding magnification factor of 50.00 kX and **b** TEOS and MCM-41 as reactants with b1 corresponding magnification factor of 50.00 kX

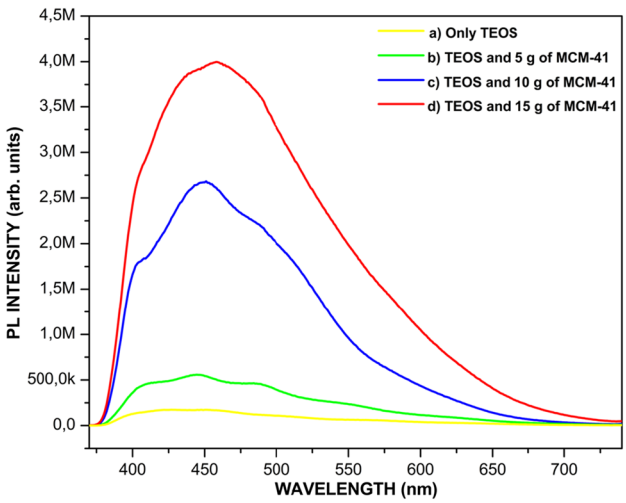

Fig. 4 Photoluminescence spectra of silicon oxycarbide thin films prepared by HFCVD using TEOS and MCM-41 as reactants

Scanning electron microscopy

In Fig. 3a, the micrograph shows a surface characterized by compact aggregates that are unevenly distributed. The formation of agglomerates is consequence of the gas-phase deposition of TEOS. In the HFCVD process, tetraethoxysilane undergoes gas-phase interactions with the hot filament, operating at a temperature of 1800 °C. During this interaction, TEOS molecules break down into reactive species. Subsequently, these reactive species undergo condensation on the substrate surface. The condensation process results in the deposition of agglomerates of silicon oxycarbide on the substrate.

The compactness and heterogeneous distribution of aggregates are attributed to variations in the nucleation and growth rates during the deposition process. The local concentration of TEOS molecules on the substrate surface, influenced by factors, such as temperature, pressure,

and gas flow rates, lead to non-uniform nucleation and subsequent growth of silicon oxycarbide aggregates.

Additionally, the interaction between TEOS molecules and the substrate surface, as well as the gas-phase reactions in the chemical vapor deposition process, contribute to the observed surface morphology. Variations in precursor adsorption, surface diffusion, and reaction kinetics result in the formation of agglomerates with different sizes and distributions across the substrate.

Figure 3a1 provides an enlarged perspective of Fig. 3a, emphasizing details with a magnification factor of 50.00 KX. This enhanced view enables the observation of microstructures, surface irregularities, and potential variations in the thickness of the thin films. Furthermore, it allows a closer examination of the surface morphology and the arrangement of clusters within the silicon oxycarbide thin film. The uneven distribution compact aggregates, which stem from TEOS decomposition products contributes to the observed surface.

Figure 3b shows the emergence of distinct clusters within the silicon oxycarbide thin film matrix, attributed to the combined use of tetraethoxysilane and MCM-41 as reactants in the Hot Filament Chemical Vapor Deposition process. The clusters exhibit a porous structure, a characteristic feature influenced by the presence of MCM-41 during deposition process [18]. The incorporation of mesoporous silica granules results in the formation of isolated groups on the film's surface, leading to the observed porous cluster morphology.

The porous clusters arise from the spatial arrangement of mesoporous silica granules, causing a non-uniform distribution on the substrate. Consequently, the silicon oxycarbide thin film shows a unique cluster morphology with a porous structure, enhancing the overall surface area. This structural variation has the potential to impact the film's mechanical, optical, and electronic properties.

Figure 3b1 provides an enhanced view of Fig. 3b with a magnification factor of 50.00 KX, focusing specifically on the intricate details of the clusters within the SiOC thin film. This micrograph highlights the presence of porous aggregates attached to the surface of larger clusters.

The observation of porous aggregates in Fig. 3b1 prompts a consideration of their potential impact on the optical properties of the SiOC thin films. The porous nature of these aggregates contributes to an increased surface area, potentially facilitating greater interaction with incident light. The network of pores within the aggregates serves as sites for charge localization, introducing variations in the electronic structure that can impact the emission characteristics of the SiOC thin film [19].

The presence of pores within the aggregates introduces a level of complexity to the electronic environment, potentially leading to localized quantum confinement effects [20]. These effects, arising from the spatial confinement of charge carriers within nanoscale dimensions, can significantly influence the band structure and, consequently, the emitted wavelengths [21].

Photoluminescence

To avoid the influence of film thickness on the analysis, each spectrum's intensity was normalized by dividing its absolute photoluminescence intensity by its corresponding thickness.

The primary feature depicted in Fig. 4 is the broad photoluminescence bands spanning from 375 to 725 nm. Notably, the sample prepared with the highest MCM-41 content exhibited the most enhanced photoluminescence intensity. This band, covering the 375 to 725 nm range, is attributed to quantum confinement effects resulting from the radiative recombination of photo-excited carriers within forbidden zone states associated with C–Si/Si–O–C bonding groups [22].

Consistent with the obtained results, a clear correlation is evident between the integrated photoluminescence intensity and the Si–O bond density. The increase in the intensity is due to the presence of a higher density of SiOx particles [23]. This phenomenon is attributed to the utilization of mesoporous silica granules and TEOS as reactants during the deposition process. Essentially, the incorporation of MCM-41 into the precursor mixture provokes an increased Si–O bond density, leading to more pronounced quantum confinement effects and, consequently, enhanced photoluminescence in the SiOC thin films.

Conclusion

The investigation into silicon oxycarbide thin films obtained by Hot Filament Chemical Vapor Deposition using tetraethoxysilane and MCM-41 as reactants has shown valuable insights into their properties and potential applications.

According to FE-SEM results, the controlled deposition of TEOS in the gas phase led to the formation of a surface characterized by compact aggregates unevenly distributed. In contrast, the combined use of TEOS and MCM-41 resulted in porous clusters, enhancing the overall surface area and introducing potential variations in optical properties.

Analysis of the chemical composition through energy-dispersive X-ray spectra confirmed the successful incorporation of carbon, oxygen, and silicon, which is consistent with the precursor materials used.

The photoluminescence spectra exhibited a broad emission band ranging from 375 to 725 nm, with the highest MCM-41 content showing the most enhanced photoluminescence intensity. This phenomenon was

attributed to quantum confinement effects, suggesting the potential for tailoring optical properties through controlled precursor usage.

The findings from this study contribute to a comprehensive understanding of the interaction between TEOS and MCM-41 in silicon oxycarbide thin-film deposition process. These outcomes hold implications for optimizing the deposition process, tailoring thin-film properties and exploring new possibilities for applications in advanced materials and device technologies. This research opens new possibilities for further exploration in diverse technological applications, spanning from microelectronics to optoelectronics.

Acknowledgments This research was made possible thanks to the generous support provided by Moscow Polytechnic University. The first author extends profound appreciation to the Consejo Nacional de Ciencia, Humanidades y Tecnología (CONAHCYT) of Mexico for awarding scholarship 573173, which significantly contributed to the successful completion of this study.

Author contributions Conceptualization: [Ivan Enrique Garcia Balderas, Alexander Petrovich Kondratov]; Methodology: [Ivan Enrique Garcia Balderas]; Formal analysis and investigation: [Ivan Enrique Garcia Balderas]; Writing and original draft preparation: [Ivan Enrique Garcia Balderas]; Writing, reviewing, and editing of the manuscript: [Ivan Enrique Garcia Balderas]; Funding acquisition: [Alexander Petrovich Kondratov]; Resources: [Alexander Petrovich Kondratov]; and Supervision: [Alexander Petrovich Kondratov].

Funding Not applicable.

Data availability Not applicable.

Declarations

Conflict of interest On behalf of all authors, the corresponding author states that there is no conflict of interest.

References

1. G.M. Renlund, S. Prochazka, R.H. Doremus, Silicon oxycarbide glasses: Part II. Structure and properties. J. Mater. Res. **6**(12), 2723–2734 (1991). https://doi.org/10.1557/jmr.1991.2723
2. P. Colombo, J.R. Hellmann, D.L. Shelleman, Mechanical properties of silicon oxycarbide ceramic foams. J. Am. Ceram. Soc. **84**(10), 2245–2251 (2001). https://doi.org/10.1111/j.1151-2916.2001.tb00996.x
3. Y.Y. Ivanova, Y.E. Vueva, Silicon oxycarbide glasses from gel hybrid structures. Adv. Mater. Res. **39–40**, 77–80 (2008). https://doi.org/10.4028/www.scientific.net/amr.39-40.77
4. N. Liao, B. Zheng, H. Zhou, W. Xue, Effect of carbon content on the structure and electronic properties of silicon oxycarbide anodes for lithium–ion batteries: A first-principles study. J. Mater. Chem. A **3**(9), 5067–5071 (2015). https://doi.org/10.1039/c4ta06932c
5. X. Yu, L. Yin, H. Lu, Y. Huo, S. Jiang, L. Zhao, B. Man, T. Ning, Third-order optical nonlinearity in silicon oxycarbide films. Opt. Mater. **104**, 109945 (2020). https://doi.org/10.1016/j.optmat.2020.109945
6. N. Liao, H. Zhou, B. Zheng, W. Xue, Silicon oxycarbide-derived carbon as potential NO_2 gas sensor: A first principles' study. IEEE Electron Device Lett. **39**(11), 1760–1763 (2018). https://doi.org/10.1109/led.2018.2869158
7. G.D. Sorarù, E. Dallapiccola, G. D'Andrea, Mechanical characterization of sol–gel-derived silicon oxycarbide glasses. J. Am. Ceram. Soc. **79**(8), 2074–2080 (1996). https://doi.org/10.1111/j.1151-2916.1996.tb08939.x
8. L. Bois, J. Maquet, F. Babonneau, D. Bahloul, Structural characterization of sol–gel derived oxycarbide Glasses. 2. Study of the thermal stability of the silicon oxycarbide phase. Chem. Mater. **7**(5), 975–981 (1995). https://doi.org/10.1021/cm00053a025
9. H. Miyazaki, Structure and optical properties of silicon oxycarbide films deposited by reactive RF magnetron sputtering using a SiC target. Jpn. J. Appl. Phys. **47**(11R), 8287 (2008). https://doi.org/10.1143/jjap.47.8287
10. M.A. Mazo, A. Nistal, A.C. Caballero, F. Rubio, J. Rubio, J.L. Oteo, Influence of processing conditions in TEOS/PDMS derived silicon oxycarbide materials. Part 1: Microstructure and properties. J. Eur. Ceram. Soc. **33**(6), 1195–1205 (2013). https://doi.org/10.1016/j.jeurceramsoc.2012.11.022
11. J. Qin, B. Li, Synthesis, characterization and catalytic performance of well-ordered crystalline heteroatom mesoporous MCM-41. Crystals (2016). https://doi.org/10.20944/preprints201612.0094.v1
12. S.V. Deshpande, J.L. Dupuie, E. Gulari, Hot filament assisted deposition of silicon nitride thin films. Appl. Phys. Lett. **61**(12), 1420–1422 (1992). https://doi.org/10.1063/1.107557
13. M. Itano, T. Kezuka, Particle adhesion and removal on wafer surfaces in RCA cleaning, in *Ultraclean Surface Processing of Silicon Wafers*. (Springer, Berlin, 1998), pp.115–136. https://doi.org/10.1007/978-3-662-03535-1_10
14. T. Hattori, Trends in wafer cleaning technology, in *Ultraclean Surface Processing of Silicon Wafers*. (Springer, Berlin, 1998), pp.437–450. https://doi.org/10.1007/978-3-662-03535-1_32
15. S.B. Desu, Decomposition chemistry of tetraethoxysilane. J. Am. Ceram. Soc. **72**(9), 1615–1621 (1989). https://doi.org/10.1111/j.1151-2916.1989.tb06292.x
16. X.S. Zhao, G.Q. Lu, X. Hu, Characterization of the structural and surface properties of chemically modified MCM-41 material. Microporous Mesoporous Mater. **41**(1–3), 37–47 (2000). https://doi.org/10.1016/s1387-1811(00)00262-6
17. S.C. Deshmukh, E.S. Aydil, Low-temperature plasma enhanced chemical vapor deposition of SiO_2. Appl. Phys. Lett. **65**(25), 3185–3187 (1994). https://doi.org/10.1063/1.112475
18. M. Broyer, S. Valange, J.P. Bellat, O. Bertrand, G. Weber, Z. Gabelica, Influence of aging, thermal, hydrothermal, and mechanical treatments on the porosity of MCM-41 mesoporous silica. Langmuir **18**(13), 5083–5091 (2002). https://doi.org/10.1021/la0118255
19. K. Lu, Porous and high surface area silicon oxycarbide-based materials—A review. Mater. Sci. Eng. R. Rep. **97**, 23–49 (2015). https://doi.org/10.1016/j.mser.2015.09.001
20. R.B. Wehrspohn, J.-N. Chazalviel, F. Ozanam, I. Solomon, Spatial versus quantum confinement in porous amorphous silicon nanostructures. The European Physical Journal B **8**(2), 179–193 (1999). https://doi.org/10.1007/s100510050681
21. Z.H. Lu, D.J. Lockwood, J.-M. Baribeau, Quantum confinement and light emission in SiO_2/Si superlattices. Nature **378**(6554), 258–260 (1995). https://doi.org/10.1038/378258a0
22. S. Gallis, V. Nikas, A.E. Kaloyeros, Silicon oxycarbide thin films and nanostructures: Synthesis, properties and applications.

Modern Technol. Creat. Thin-Film Syst. Coat. (2017). https://doi.org/10.5772/66992
23. ZSh. Shaymardanov, S.S. Kurbanov, RYu. Rakhimov, The effect of packing density on luminescence of amorphous SiO_2 nanoparticles. Opt. Spectrosc. **120**(6), 922–925 (2016). https://doi.org/10.1134/s0030400x16060205